



# Modeling and experimental validation of cellular porous material with large resonant inclusions

Olivier DOUTRES<sup>1</sup>; Noureddine ATALLA<sup>2</sup>; Haisam OSMAN<sup>3</sup>

<sup>1,2</sup>GAUS, Canada

<sup>3</sup>ULA, United States of America

## ABSTRACT

Porous materials are widely used for improving sound absorption and sound transmission loss of vibrating structures. However, their efficiency is limited to medium and high frequencies. A common solution for improving their low frequency behavior while keeping an acceptable thickness is to embed resonant structures such as Helmholtz resonators. This work investigates the absorption and transmission acoustic performances of a cellular porous material with large resonator inclusions. The homogenization theory cannot be applied to cellular material made of such large periodic unit-cell (e.g., cube of side  $L \approx 100$  mm). A low frequency model of a large resonant unit-cell based on the Parallel Transfer Matrix Method is proposed in this work. The proposed model is validated by comparison with impedance tube measurements and finite element calculations. At the Helmholtz resonance frequency; (i) the transmission loss is greatly improved and (ii) the sound absorption of the host material is decreased if it is made of a highly sound absorbing material.

Keywords: Porous material, low frequency, Helmholtz resonator, metamaterial, sound transmission loss, sound absorption

## 1. INTRODUCTION

A low frequency solution to improve the acoustic efficiency of passive open-cell porous materials is to embed Helmholtz resonators (HR) in the porous matrix. One of the first works describing such structure is a patent filed in by Borchers et al. [1] in which a resonant acoustic protection is proposed to attenuate low frequency noise level inside payload fairings of launch vehicles. Much later, Sugie et al. [2] proposed a similar heterogeneous material made of a fibrous sound absorbers with resonant inclusions in order to improve the low frequency sound transmission loss of double-leaf structures at the mass-air-mass resonance frequency. More recently, the acoustic community had shown a keen interest in this type of resonant structure since the equivalent material (also called effective material or metamaterial) presents a negative bulk modulus at the HR resonance frequency [3,4]. Most of these works mainly focused on the transmission properties of the resonant material and highlighted the large transmission dip at the HR resonance frequency [3]. Lagarrigue et al. [5] recently investigated the sound absorption efficiency of rigid backed acoustic foams with resonant split hollow cylinder inclusions and shown that it is greatly improved for frequencies with wavelength much larger than the material thickness. Under the assumption that the HR periodicity is much smaller than the acoustic wavelength, the resonant materials are usually modelled as homogenized equivalent material with modified bulk modulus to account for the presence of the resonant inclusion [3,4,6]. The analytical expression of the equivalent bulk modulus originally proposed by Fang et al. [4], has been extended by Boutin [6] for HRs embedded in a foam matrix using the homogenization method.

Cellular resonant material with large periodicity obviously prevents the use of the homogenization method. In this case, the orientation of the HR neck may have a strong influence on the sound absorption behavior of the resonant material [5]. The work presented in this paper deals with the

---

<sup>1</sup> olivier.doutres@usherbrooke.ca

<sup>2</sup> noureddine.atalla@usherbrooke.ca

<sup>3</sup> haisam.a.osman@ulalaunch.com

analytical modeling and the experimental validation of cellular resonant porous material made of large periodic unit-cell (PUC) with a spherical Helmholtz resonator inclusion (PUC dimensions are around  $100 \text{ mm} \times 100 \text{ mm} \times 100 \text{ mm}$ ). The HR lies in the center of the PUC and can be completely buried or not. A model based on an augmented transfer matrix method [7] (referred to as P-TMM) is proposed here. The normal incidence acoustical behavior of the resonant PUC is thus modeled by a combination of porous element in series, and parallel elements to account for the HR inclusion. Both the sound absorption and the sound transmission loss behaviors are investigated and focus is put on the effect of the HR orientation within the foam matrix.

## 2. TRANSFER MATRIX MODELING OF THE PUC

The proposed cellular material is defined as an arrangement of a rectangular Periodic Unit-Cells (PUC); as shown in Fig. 1(a). The PUC is composed of a large Helmholtz Resonator (HR) embedded in a porous substrate (i.e., PUC side  $L \geq 80 \text{ mm}$  and HR cavity diameter  $\geq 60 \text{ mm}$ ). For such large PUC, the scale separation between the macroscopic characteristic length of the wave  $\lambda/(2\pi)$  and the PUC size  $L$ , i.e.  $L \ll \lambda/(2\pi)$ , is not respected which prevents the use of the homogenization method to derive the macroscopic properties of an equivalent fluid by means of multiple scale expansions [6]. The Parallel Transfer Matrix Method (P-TMM) [7] is used in this work to model the one dimensional acoustical behavior of large resonant PUC. In this approach, the PUC is modeled as a stack in series of three layers of thickness  $l_1$ ,  $l_2$  and  $l_3$  ( $l=l_1+l_2+l_3$ ). Layers 1 and 3 are homogenous foams while layer 2 (the middle layer) is a parallel assembly of the HR and the foam matrix. Since in our testing (see sections 4 and 5), the resonators are spherical, the middle layer was first perforated before embedding the HR. This creates a thin air gap behind the resonators. This is taken care of in the model by adding a thin layer of thickness  $l_{2a}$  made up from air and foam in parallel (see Figs. 1(c) and 1(d)). The sub-layer containing the HR, called “2HR”, combines the transfer matrix of the porous layer and the one of the HR. Its thickness (i.e.,  $l_{2HR}$ ) is set to the thickness of the HR cavity being an equivalent cylinder with the same volume as the spherical HR and the circular cross-section area of the perforation.

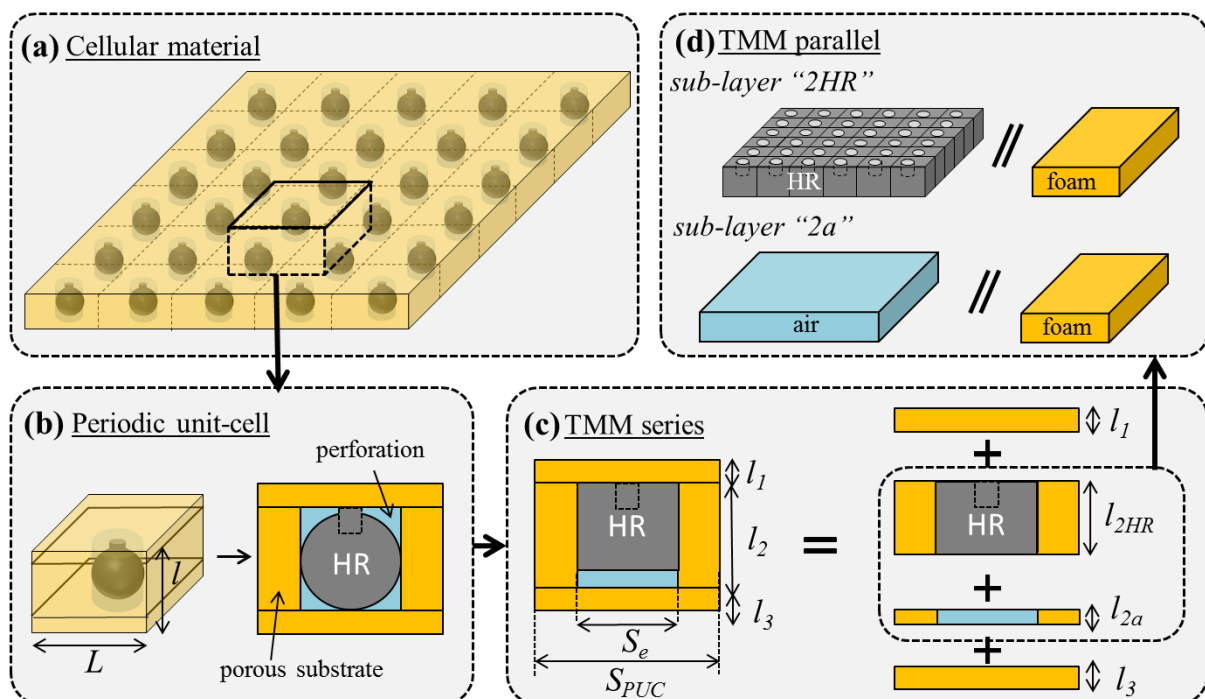


Figure 1 – Scheme of the cellular material.

The transfer matrix of the PUC presented in Fig. 1(c) is given by

$$\begin{aligned} T^{PUC} &= \begin{bmatrix} T_{11}^{PUC} & T_{12}^{PUC} \\ T_{21}^{PUC} & T_{22}^{PUC} \end{bmatrix} = T^{layer,1} \times T^{layer,2} \times T^{layer,3} \\ &= T^{layer,1} \times T^{layer,2HR} \times T^{layer,2a} \times T^{layer,3} \end{aligned} \quad (1)$$

All porous materials are modeled using the equivalent fluid model [8] and thus can be represented by a  $2 \times 2$  transfer matrix. The transfer matrices of the two outer homogeneous porous layers  $T^{layer,i}$  (with  $i=1$  and  $3$ ) are well known and equal to

$$T^{layer,i} = \begin{bmatrix} T_{11}^i & T_{12}^i \\ T_{21}^i & T_{22}^i \end{bmatrix} = \begin{bmatrix} \cos(k_{eq,i}l_i) & jZ_{eq,i} \sin(k_{eq,i}l_i) \\ j \sin(k_{eq,i}l_i) / Z_{eq,i} & \cos(k_{eq,i}l_i) \end{bmatrix}, \quad (2)$$

with  $k_{eq,i}$  and  $Z_{eq,i}$  the wave number and characteristic impedance of the equivalent fluid, respectively.

The transfer matrix of layer 2 combines two sub-matrices  $T^{layer,2HR}$  and  $T^{layer,2a}$  which are modeled using a parallel assembly as proposed by Verdière *et al.* [7]. According to these authors, the following conditions must be fulfilled if ones want to use P-TMM: (1) only plane waves propagate upstream and downstream of the periodic construction; (2) only normal incidence plane waves propagate in the construction; (3) no pressure diffusion exists between adjacent parallel elements, (4) the wavelength is much larger than the PUC, and (5) each element can be represented by a  $2 \times 2$  transfer matrix. Conditions (2) to (5) are fulfilled here since we consider (i) low frequencies, (ii) porous frame with intermediate airflow resistivity, (iii) equivalent fluid models for predicting their acoustic behavior and finally, (iv) HR which are known to behave as locally reacting elements. However, assumption (1) seems physically unrealistic around the HR resonance frequency and some discrepancies between simulations and measurements are expected.

For both sub-layers “2HR” and “2a”, the transfer matrix is given by

$$T^{layer,2m} = \frac{-1}{\sum r_n Y_{21}^n} \begin{bmatrix} \sum r_n Y_{22}^n & -1 \\ \sum r_n Y_{11}^n - \sum r_n Y_{12}^n \sum r_n Y_{21}^n & -\sum r_n Y_{11}^n \end{bmatrix}, \quad (3)$$

with  $m=HR$  or  $m=a$  and  $n=mat$  for the porous substrate and  $n=m=HR$  (resp.,  $n=a$ ) for the resonator element (resp., air layer).  $r_n$  is the surface ratio of each element and is identical for the two matrices  $T^{layer,2m}$  since they share the same perforation diameter. Knowing the surface of the resonator  $S_e$ , and the surface of the unit cell  $S_{PUC}$  (see Fig. 1(c)), thus  $r_{HR}=r_a=r= S_e / S_{PUC}$  and  $r_{mat}=1- r$ . The admittance matrix for each element are given by

$$Y^n = \begin{bmatrix} Y_{11}^n & Y_{12}^n \\ Y_{21}^n & Y_{22}^n \end{bmatrix} = \frac{1}{T_{12}^n} \begin{bmatrix} T_{22}^n & T_{21}^n T_{12}^n - T_{22}^n T_{11}^n \\ 1 & -T_{11}^n \end{bmatrix}. \quad (4)$$

The transfer matrices of the material and of the air layer  $T^n$  (i.e.,  $n=mat$  and  $n=a$ ) are calculated by using Eq. (2). In the case of the air layer,  $Z_{eq,i}$  has to be replaced by  $Z_0$ ,  $k_{eq,i}$  by  $k_0$  and  $l_i$  by  $l_{2a}$ . The transfer matrix of the resonator  $T^{HR}$  (i.e.,  $n=HR$ ) is the one of a resonator array as described in refs. [8] and [9]. It is written as a product of the inertial and acoustic components [9]. For an acoustic wave impinging on the neck side of the HR (this HR position is called **AB** in this paper), its transfer matrix is given by

$$T^{HR,AB} = \begin{bmatrix} 1 & 0 \\ 1/Z_A & 1 \end{bmatrix} \begin{bmatrix} 1 & j\omega M \\ 0 & 1 \end{bmatrix}, \quad (5)$$

with  $M$  the mass per unit area of the resonator array and  $Z_A$  the acoustic input impedance. The reader is referred to reference [8] (page 203) for a complete description of the calculations related to  $Z_A$ . Finally, various acoustic features can be determined from the transfer matrix of the PUC given by Eq. (1). It is worth noting that the combination of Eqs. (1), (3) and (5) stands for an acoustic wave impinging on the neck side of the HR (i.e., position **AB**). The transfer matrix of the PUC in the opposite direction **BA**, i.e. the PUC is inverted and the acoustic wave now impinges on the rear side of the HR, can be obtained by simply inverting the matrix of Eq. (1) accounting for a change in the sign of the velocity by  $-u$  [10].

### 3. VALIDATION

The normal incidence behavior of a large PUC is investigated both analytically (P-TMM), numerically (FEM) and experimentally.

The PUC investigated in this work has a large spherical HR of 58 mm inner diameter embedded in its center (see Fig. 1(b)). The HR neck is cylindrical with a depth of 7 mm and an inner radius of 4.6 mm. The Helmholtz resonance frequency  $f_0$  is 383 Hz. The host material is made of 4 in. ultra-light melamine. It is modeled as an equivalent fluid using the properties in table 1. The Melamine matrix is made of three layers: layer 1 (when used) is ½ in.-thick, layer 2 is 3 in.-thick and layer 3 is 1 in.-thick. It is worth mentioning that similar tests have been carried out successfully with HRs tuned to 150 Hz. However, these results are not shown here for conciseness.

Table 1 – Non-acoustic parameters of the host material

	Airflow		Viscous	Thermal	Frame
Porosity	resistivity (N.s.m <sup>-4</sup> )	Tortuosity	characteristic length (μm)	characteristic length (μm)	density (kg.m <sup>-3</sup> )
0.996	7300	1	88	160	5.5

Both the normal incidence sound absorption coefficient  $\alpha$  and normal incidence sound transmission loss  $TL_n$  are measured and compared to the proposed P-TMM simulations. The unit-cell considered in this section is cylindrical since its acoustical behavior is investigated using a cylindrical impedance tube. The two acoustic indicators are measured according to standard ASTM E1050-10 [11] and standard ASTM E2611-09 [12] adapted to the three microphone method [13] using a cylindrical 100 mm diameter impedance tube (see Fig. 2). The foam matrix of the cylindrical PUC is made of layer 2 and 3 ( $l=4$  in.) and includes the HR in the center of layer 2. The surface ratio in this case is  $r=36\%$ . Measurements are presented in Fig. 3 and compared to simulations either performed with the rigid frame or the limp frame model for the porous matrix [8].

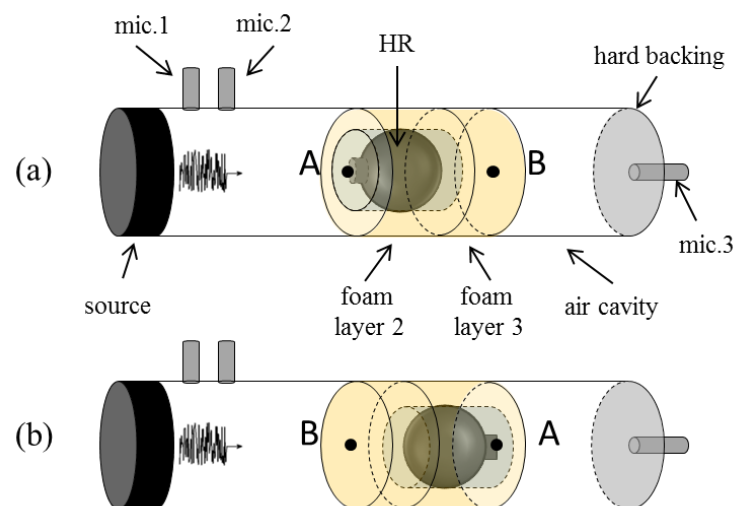


Figure 2 – Schematic of the impedance tube test; (a) PUC in position **AB**, (b) PUC in position **BA**.

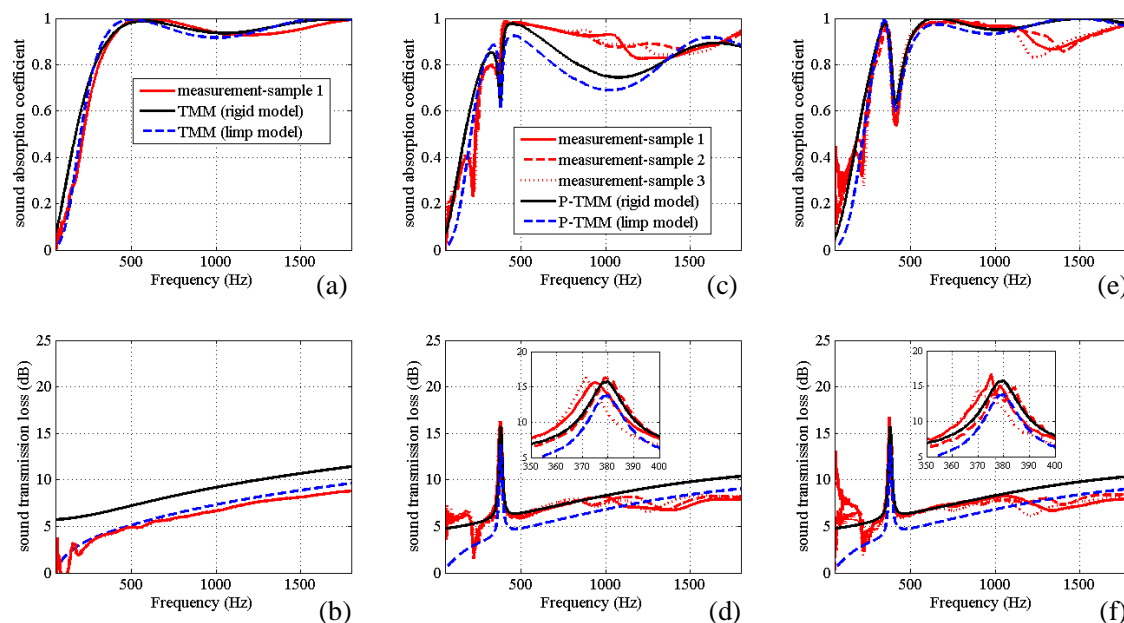


Figure 3 – Impedance tube measurements versus P-TMM simulations: (first line) sound absorption coefficient of the PUC backed by a 1 in. thick air cavity, (second line) sound transmission loss; (first column) homogeneous foam, (second column) PUC in position **AB**, (third column) PUC in position **BA**.

Figs. 3(a) and 3(b) present the acoustic features of the melamine sample (no HR, no perforation). It is shown that both the rigid and the limp assumptions correctly estimate the sound absorption behavior. However, the limp assumption should be preferred to predict the transmission behavior of the porous matrix. The HR is now inserted in the porous matrix and the acoustic behavior of the PUC is measured either in the **AB** position (see Fig. 3(c) and 3(d)) or the **BA** position (see Fig. 3(e) and 3(f)). Three dips can be observed in the measured sound absorption curves (see red curves). The first one, occurring around 220 Hz, and the third one, occurring around 1300 Hz, are attributed to mechanical resonances of the porous matrix. These two mechanical resonances also affect the transmission loss as shown in Figs. 3(d) and 3(f). The second sound absorption dip occurs around the HR resonance frequency  $f_0$  (i.e. 375 Hz) in the **AB** position and slightly above  $f_0$  (i.e., 400 Hz) in the **BA** position. It can be observed that the sound absorption dip is more pronounced in the latter position. Above 500 Hz, the sound absorption efficiency in position **BA** is greater than the one in position **AB**. The asymmetry observed between positions **AB** and **BA** clearly indicates that the PUC cannot be modeled according to the homogenization theory since its acoustic behavior depends on the orientation of the HR' neck inside the PUC. Furthermore, a decrease of the sound absorption efficiency of the PUC at the HR resonance is quite unexpected since HRs are usually used to improve this acoustic property. Simple analytical calculations (not shown here for conciseness) prove that the acoustic behavior at the HR resonance frequency  $f_0$  is controlled by the HR component of the parallel assembly: the sound absorption efficiency of the parallel assembly is thus decreased if the sound absorption efficiency of the HR alone is inferior to the one of the host material.

A sound transmission peak with high amplitude (~9 dB) but relatively narrow band is observed at the HR resonance frequency (see Figs. 3(d) and 3(f)). This peak is related to a negative group velocity and negative bulk modulus of the equivalent metamaterial [4].

P-TMM simulations (black and blue curves) do not predict the dips related to mechanical resonances since the equivalent fluid assumption is used to model the foam matrix. The rigid frame model better captures the acoustic properties of the resonant PUC (Figs. 3(d) and 3(f)) since the HR insertion exerts a lateral compression and stiffens artificially the material. Both the sound absorption dip and sound transmission peak associated to the HR resonance frequency are correctly predicted in both positions **AB** and **BA**. The main discrepancy between measurements and P-TMM simulations arises in the sound absorption coefficient in position **AB** for frequencies just above  $f_0$ . The P-TMM underestimates the sound absorption coefficient since it does not account for the air layer in front of the spherical HR.

To explain this point, the impedance tube measurements were numerically reproduced using the commercial FEM software COMSOL® Multiphysics. Figure 4 shows the simulated configuration. A unit pressure is applied on the source side to simulate the normal incidence excitation. The HR walls are modeled as impervious, rigid and motionless. The JCA equivalent fluid rigid model is used here for the host foam material and for the air layer situated in the HR neck to account for viscous and thermal dissipations. The effective properties of the air in the HR neck are computed using a cylindrical pore model. Because the proposed P-TMM model does not take into account the air layer inside the spherical perforation (made to host the HR) and above the HR front face, the FEM simulations are carried out with two different conditions at the perforation/foam interface  $S_c$  as shown in Fig. 4: (i) open and (ii) impervious and rigid. The latter configuration is referred to as the semi/open configuration and is supposed to mimic the P-TMM modeling.

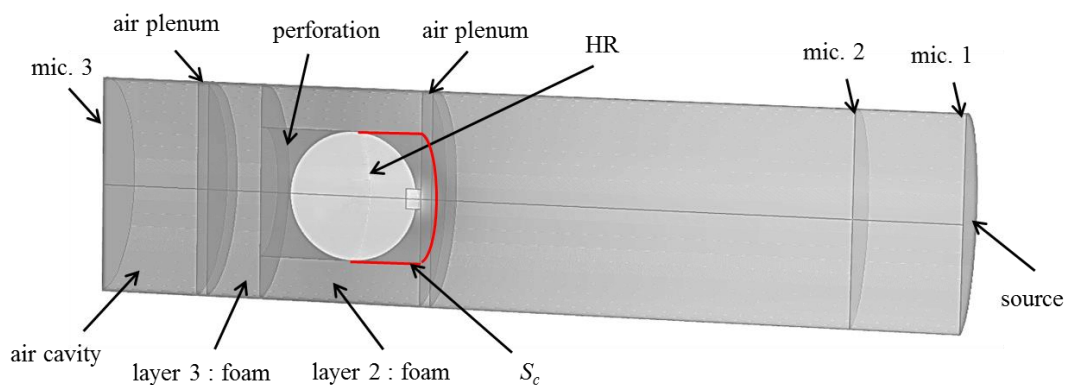


Figure 4 – 2D FEM model of the impedance tube configuration.

Figure 5 shows very good agreement between the proposed P-TMM model of the resonant PUC and the FEM simulations. However, the amplitude of the dip (resp. peak) in the FEM obtained sound absorption curve (resp. sound transmission loss curve) at the HR resonance is more pronounced compared to P-TMM and is also slightly shifted toward higher frequencies. Since the P-TMM successfully simulates the measured acoustic features at the HR resonance frequency as shown in Fig. 3, the differences between P-TMM and FEM at this frequency is more likely due to an inaccuracy in the FEM simulation. However, this was not investigated.

The FEM simulation of the sound absorption of the PUC in position **AB** is in better agreement with P-TMM above 400 Hz when surface  $S_c$  is replaced by an impervious wall (see blue squares in Fig. 5(c)). This confirms that the underestimation of the sound absorption in position **AB** observed between P-TMM and impedance tube measurements can partly be attributed to sound absorption at the perforation walls in front of the HR. The semi/close FEM configuration is also associated to a slight increase in sound transmission loss (< 1 dB). This is expected since more acoustic energy has been reflected at the upstream face of the PUC.

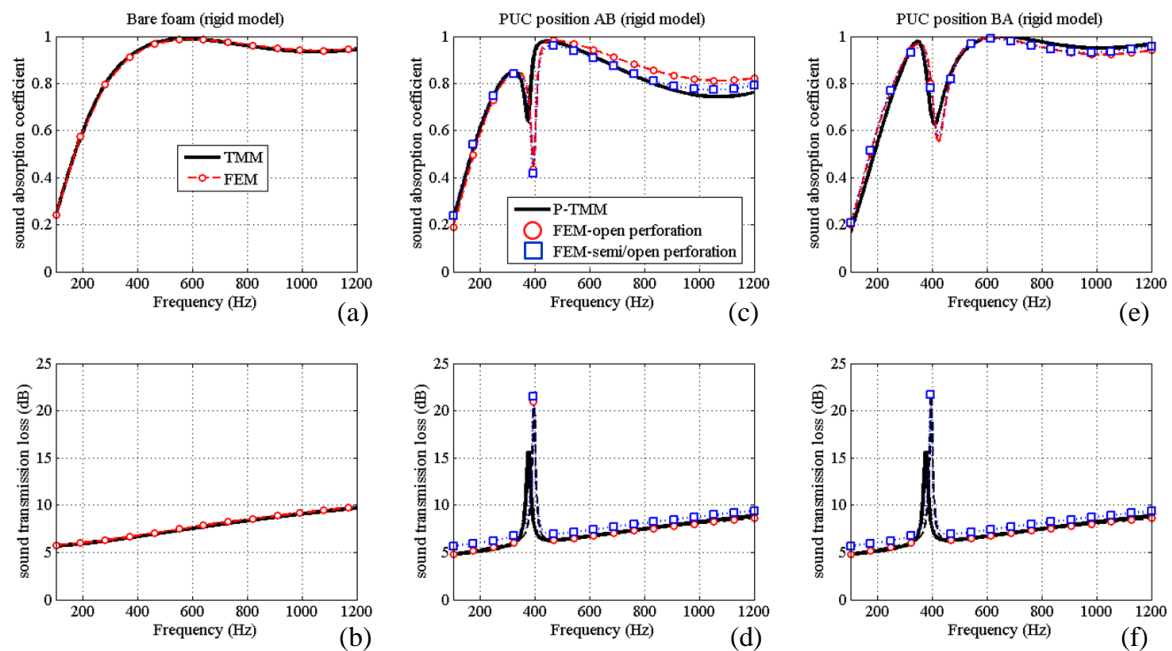


Figure 5 – P-TMM versus FEM: (first line) sound absorption coefficient of the PUC when backed by a 1 in. thick air cavity, (second line) sound transmission loss. (first column) homogeneous foam, (second column) PUC in position **AB**, (third column) PUC in position **BA**;

#### 4. CONCLUSIONS

In this work, the acoustic properties of a cellular porous material with large resonant inclusions have been investigated analytically, numerically and experimentally. Since the characteristic dimensions of the periodic unit cell does not allow the use of the homogenisation method, a model based on the transfer matrix method is proposed to model the normal incidence acoustic properties of the resonant material. It is shown that the transmission loss of the material is greatly improved at the HR resonance frequency. However, the HR contributes negatively to the sound absorbing efficiency of the porous host material at the HR resonance frequency and this decrease is shown to depend on the HR neck orientation within the material. All these acoustic features associated to the HR inclusion and which depend on the HR orientation within the porous substrate are correctly predicted by the proposed P-TMM model.

#### ACKNOWLEDGEMENTS

The authors would like to thank the National Sciences and Engineering Research Council of Canada (NSERC) for providing financial support.

#### REFERENCES

1. Borchers IU, Laemmlin ST, Bartels P, Rausch A, Faust M, Coebergh JAF, Koeble K, Acoustic protection on payload fairings of expendable launch vehicles. U.S. Patent 1997; No. 5,670,758.
2. Sugie S, Yoshimura J, Iwase T, Effect of inserting a Helmholtz resonator on sound insulation in a double-leaf partition cavity, *Acoustical Science and Technology* 2009; 30(5): 317-326.
3. Ding CL, Hao L, Zhao XP. Two-dimensional acoustic metamaterial with negative modulus, *J Appl Phys* 2010; 108: 074911.
4. Fang N, Xi D, Xu J, Ambati M, Srituravanich W, Sun C, Zhang X. Ultrasonic meta-material with negative modulus. *Nature Materials* 2006; 5:452–456.
5. Lagarrigue C, Groby JP, Tournat V, Dazel O. Absorption of sound by porous layers with embedded periodic arrays of resonant inclusions. *J Acoust Soc Am* 2013; 134(6) Pt. 2: 4670-4680.
6. Boutin C, Acoustics of porous media with inner resonators, *J Acoust Soc Am* 2013; 134(6) Pt. 2:4717-4729.

7. Verdière K, Panneton R, Elkoun S, Dupont T, Leclaire P. Transfer matrix method applied to the parallel assembly of sound absorbing materials. *J Acoust Soc Am* 2013; 134(6):4648.
8. Allard JF, Atalla N. *Propagation of sound in porous media: Modeling sound absorbing materials*, 2nd ed. Wiley, 2009.
9. Efmitsov BM, Lazarev LA. Sound transmission loss of panels with resonant elements. *Acoustical Physics* 2001; 47(3): 346-351.
10. Panneton R. Normal incidence sound transmission loss evaluation by upstream surface impedance measurements. *J Acoust Soc Am* 2009; 125(3): 1470.
11. Anonymous. Standard test method for impedance and absorption of acoustical materials using a tube, two microphones and a digital frequency analysis system. American Society for Testing and Materials ASTM E1050-10.
12. Anonymous. Standard test method Measurement of Normal Incidence Sound Transmission of Acoustical Materials Based on the Transfer Matrix Method. American Society for Testing and Materials ASTM E2611-09.
13. Salissou Y, Panneton R, Doutres O. Complement to standard method for measuring normal incidence sound transmission loss with three microphones. *J Acoust Soc Am* 2012; 131 EL216–EL222.